

Threshold behaviours in $\text{Ge}_x\text{As}_{10}\text{Se}_{90-x}$ and $\text{Ge}_x\text{Sb}_{10}\text{Se}_{90-x}$ glasses

S. W. Xu*, T. W. Liang

*College of Mathematics and Physics, Hunan University of Arts and Science,
415000, Changde, People's Republic of China*

We investigated the effect of the elemental substitution of As by Sb on the threshold behaviours in $\text{Ge}_x\text{As}(\text{Sb})_{10}\text{Se}_{90-x}$ glasses. We found that, while the transition thresholds at $\text{MCN}=2.4$ and 2.67 were verified in the GeAsSe glasses, the transition thresholds can be changed to chemically stoichiometric compositions if As is substituted by Sb. We further deconvolved Raman spectra into different structural units and the change of their respective intensity showed the same behaviour, and this was ascribed to the chemical effect induced by a large difference of the atomic radius between As and Sb, and a relatively strong ionic feature of the element Sb.

(Received September 7, 2023; Accepted November 13, 2023)

Keywords: Chalcogenide glasses, Transition thresholds, Raman spectra

1. Introduction

Chalcogenide glasses consist of one or more of the chalcogen elements S, Se and Te covalently bonded to other elements such as Ge, As, or Sb, etc. They have many unique properties including low phonon energy, broad transmission window, ultrafast optical response time, and high linear and nonlinear refractive index, and making the glasses very useful in infrared optics and photonics [1-6]. Moreover, these properties can be easily tuned in a widely compositional range, since the glass-forming region is broad. Therefore, it is flexible to design the material compositions tailoring any particular device application.

To explain why the properties in chalcogenide glasses change with the glass composition, two different models have been proposed. One is the chemically ordered covalent network (COCN) [7,8] and another is the topological model based on constraint theory [9,10]. In the COCN model, heteropolar bonds are dominated and thus the chemical order is preserved. Therefore, physical parameters in the extremum or a change in slope can be found at the stoichiometric or tie-line compositions in the glasses, and this usually is called the chemical thresholds of the glasses. On the other hand, mean coordination number (MCN), defined as a sum of the content of each element in the glass times its coordination number, is quite often used as an estimation of the glass network connectivity in the topological model. The transition usually is observed at $\text{MCN}=2.4$ from an under-constrained network to an over-constrained phase [9,10], A second phase transition existed at $\text{MCN}=2.67$ corresponding to a topological change from a 2-D to 3-D “stressed rigid” phase [11]. Many chemical and physical properties have been found to change abruptly at these transition thresholds in various glass compositions. For instance, various physical parameters, like material density; elastic moduli; index of refraction; band-gap, etc, showed clear transition at these thresholds in the literatures [12-16].

While both models can partly explain the compositional dependence of the physical properties, it is obvious that the chemical order should be violated in extremely chalcogen-poor glasses where many homopolar bonds like Ge-Ge or As-As should appear. On the other hand, it has been found that the transition behaviors are not always located at $\text{MCN}=2.67$ as predicted by the topological model [17]. The questions are thus raised: to which degree these two models can be valid to explain the compositional dependence of the properties in the glasses? And how can the chemical composition affect the threshold behaviors in the glasses?

* Corresponding author: xusiwei1227@163.com
<https://doi.org/10.15251/CL.2023.2011.829>

To answer these, in the present paper we measured the evolution of physical properties in GeAsSe and GeSbSe glass systems, where As or Sb contents were fixed at 10%, and Ge content was changed from 5% to around 30%. This could help us understand how the chemical composition and MCN, and how the elemental substitution can affect the properties of the glasses. The glass transition temperature, density, refractive index and optical bandgap, were measured and Raman spectra of the glasses were further recorded to understand the correlation between the change of the glass structure and properties. We found, while the MCN was dominated in tuning the properties of the glasses, chemical compositions became increasingly important especially in the GeSbSe glasses deviated from ideally covalent network.

2. Experimental

$\text{Ge}_x\text{As}(\text{Sb})_{10}\text{Se}_{90-x}$ bulk glasses with an MCN from 2.2 to 2.9 were prepared by the melt-quenching method. The details on the preparation conditions are similar to those in the previous literatures [17]. The glass rods were cut into the discs with a diameter of 10 mm and a thickness of 1 mm. The discs were further polished with two parallel optical surface. No any observable bubbles or impurities can be found using an infrared microscope. An energy dispersive x-ray spectrometer (EDX) installed on a scanning electron microscope was used to measure the chemical compositions of the glasses. In all cases, the measured composition had less than 0.3 mol% different from the corresponding nominal one. All the glasses are amorphous as confirmed by x-ray diffraction (XRD) method. Glass transition temperature T_g was measured by a differential scanning calorimeter (Mettler-Toledo, DSC 1), and the refractive index was measured using a Metricon Model 2010 prism coupler. For Raman scattering measurements, 830 nm laser line with 0.1 mW power was used to excite Raman spectra. The glass density ρ was measured using the Archimedes principles, and each glass composition were measured five times to get the average density.

3. Results and discussion

The coordinated number of Ge, As(Sb) and Se are 4, 3 and 2, respectively, in chalcogenide glasses[1,2].Therefore, MCN of $\text{Ge}_x\text{As}(\text{Sb})_{10}\text{Se}_{90-x}$ is $[4x+3\times 10+2\times(90-x)]/100=2.1+0.02x$. Obviously there is a one-to-one correspondence between Ge concentration and MCN. Below we show all the physical parameters as a function of MCN and this is easily converted into Ge concentration based on the formula above.

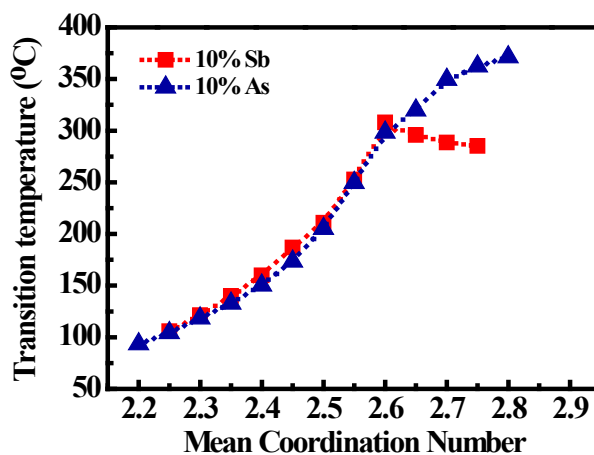


Fig. 1. The correlation between glass transition temperature T_g and MCN

Fig. 1 shows the correlation between T_g and MCN, where T_g increases almost linearly with the increase of MCN in GeAsSe glasses, and this is in contrast with that in GeSbSe glasses where a maximum T_g appears at the chemically stoichiometric composition for each curve. Since T_g reflects the degree of the glass network connectivity [18], the appearance of the global maximum indicates that the glass network is destroyed with increasing MCN in the GeSbSe glasses.

Fig. 2 is the relation between the density of the glasses and MCN. Due to larger atomic weight of Sb compared with that of As, the density in GeSbSe glass is larger than that of the corresponding GeAsSe glass. A minimum density at MCN=2.67 can be verified while a slight trace of the transition of the maximum at MCN=2.4 can be observed in GeAsSe glasses. However, a minimum density can be found at MCN=2.60 in GeSbSe glasses which corresponds to the chemically stoichiometric $\text{Ge}_{25}\text{Sb}_{10}\text{Se}_{65}$.

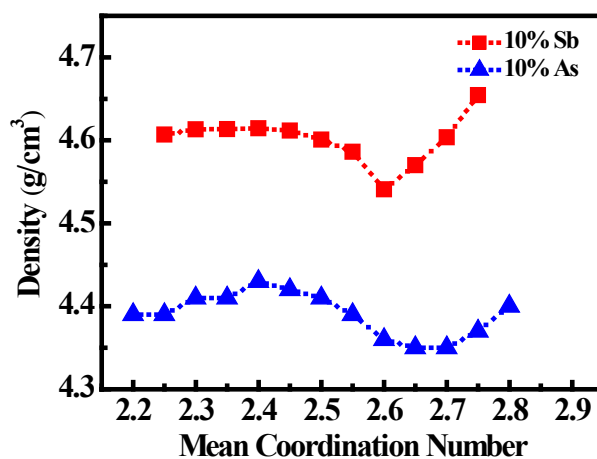


Fig. 2. Density of the glass as a function of MCN

Each atomic weight in GeAsSe glass is slightly different. Supposing that the atomic arrangement keeps unchanged in GeAsSe glasses with a fixed As content of 10%, then substitution of Se by Ge could lead to a small density since Se is heavier than Ge. The present results in Fig. 2 is opposite to the expectation, especially in the MCN below 2.4 and above 2.6, the increasing density with MCN implies significant changes in the atomic arrangement. The similar change can be observed in GeSbSe glasses, although there is no clear signals of the maximum at MCN=2.4 in Fig. 2. However, these two groups of the glasses exhibit slightly different in their transition thresholds, suggesting that chemical composition might affect the structure of the glass system.

Fig. 3 shows the refractive index of the glasses as a function of MCN. Once again, we observed that, while the minimum of the refractive index appears at MCN=2.67 for GeAsSe glasses, its value changes to MCN=2.6 for the $\text{Ge}_x\text{Sb}_{10}\text{Se}_{90-x}$ glasses.

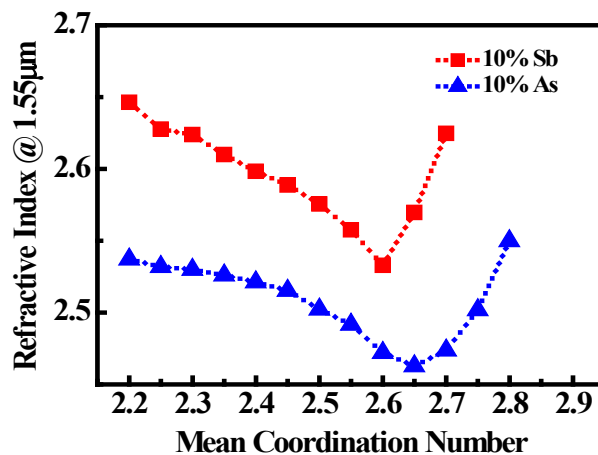


Fig. 3. The relation between refractive index of the glass and MCN.

We measured Raman spectra of the glasses in order to understand how the change of the glass structure can affect the transition thresholds in Ge-As(Sb)-Se glasses. Fig. 4(a) and (b) show Raman spectra of GeAsSe and GeSbSe glasses, respectively. All the spectra exhibit broad bands from 150 cm^{-1} to 350 cm^{-1} . It is well accepted that, the cross-link of the substructural units like $\text{GeSe}_{4/2}$ tetrahedral, $\text{As(Sb)Se}_{3/2}$ pyramidal and some homopolar Ge-Ge, As-As(Sb-Sb), Se-Se bonds forms Ge-As-Se glass network. Raman vibrations at 195 cm^{-1} and 215 cm^{-1} correspond to the corner-sharing (CS) and edge-sharing (ES) $\text{GeSe}_{4/2}$ tetrahedral units, respectively [17,18]. The peak around at 230 cm^{-1} was ascribed to pyramidal $\text{AsSe}_{3/2}$ modes. $\text{SbSe}_{3/2}$ pyramids were reported to have a feature at 195 cm^{-1} , but obviously this was hidden behind the broad $\text{GeSe}_{4/2}$ bands due to the overlapping of broad vibrational bands in the glasses [17,19]. The peak at 250 cm^{-1} was due to the vibrational modes in the Se chains or rings [7,19]. In addition, it was natural expected that the number of so-called wrong bonds of Ge-Ge, As-As and Sb-Sb, becomes larger with the increase of Ge concentration. The peaks at 175 cm^{-1} and 300 cm^{-1} were characteristic of the Ge-Ge mode of the ethane-like $(\text{Se}_2)\text{Ge}=\text{Ge}(\text{Se}_2)$ structural units, and Sb-Sb vibrations were found at 160 cm^{-1} [17,19-22].

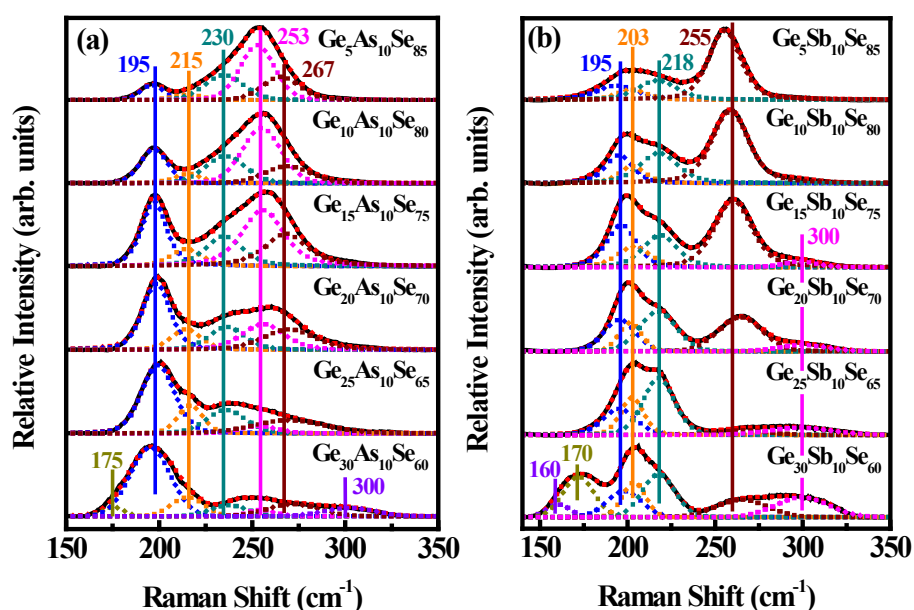


Fig. 4. Raman spectra of $\text{Ge}_x\text{As}_{10}\text{Se}_{90-x}$ (a) and $\text{Ge}_x\text{Sb}_{10}\text{Se}_{90-x}$ (b) glasses and their decompositions.

We decomposed Raman spectra of these glasses into these different structural units following the assignments mentioned above, as shown in Fig. 4, and considered the integrated area of each substructural units to the whole spectral area as the content of each substructural unit. Fig. 5 (a) and (b) show the content of each structural units as a function of MCN in GeAsSe and GeSbSe glasses, respectively. For GeAsSe glasses, all the change of the content of the different structural units exhibits a transition at MCN=2.67, while for the GeSbSe glasses, the transition occurs at the chemically stoichiometric composition.

For GeAsSe glasses, different elements are next to each other in the Periodic Table and thus their atomic radii and electronegativity are relatively close, hence GeAsSe glasses were usually considered as an ideal covalent network system to examine the rigidity percolation theory. In GeAsSe glasses, the mismatching between the different atoms can be well suppressed, and thus the observed transition thresholds at MCN=2.4 and 2.67 are in agreement with the predictions by the mean field theory. In contrast, physical parameters exhibit extrema at the chemically stoichiometric GeSbSe glass. The difference may come from the large mismatching in atomic radius, or relatively strong ionic feature of the Sb element. In fact, the similar chemical effects can be observed in GeGaS and GeSbS glasses with such large mismatching [23,24].

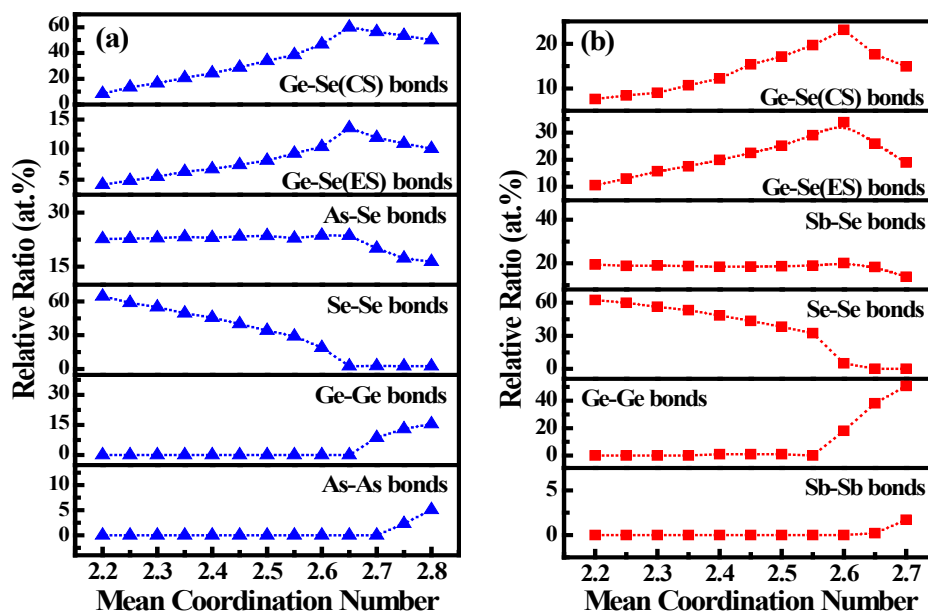


Fig. 5. The content of different structural units as a function of MCN in $Ge_xAs_{10}Se_{90-x}$ (a) and $Ge_xSb_{10}Se_{90-x}$ (b) glasses.

Recently, Opletal et.al. simulated the structure of GeAsSe and GeSbSe glasses, the initial configurations of 240 atoms consisting of the glasses were generated via the Reverse Monte Carlo method before being temperature quenched via ab-initio molecular dynamics simulations [25]. It was found that the appearance of the extrema in physical parameters was accompanied with a maximum number of Ge(As/Sb)-Se-Ge(As/Sb) units in the network. This corresponds to the chemical stoichiometric compositions in the GeSbSe system, but the minimum in the refractive index and the maximum content of Ge(As)-Se-Ge(As) units appear at MCN = 2.67 in the GeAsSe system. Further structural analysis indicated that, As-As-Se₂ units appear at the cost of As-Se₃ units, resulting in an increase to homopolar bonding beyond the transition in GeAsSe glasses, but the similar situation with Sb-Sb-Se₂ units was never observed in the GeSbSe system. The results are in agreement with those in Fig. 5.

The present results verify that, the constraint theory with the transition thresholds at MCN=2.4 and 2.67 is valid in an ideally covalent system like GeAsSe glasses, but this could be violated in non-ideal systems like GeSbSe and GeGaS glasses, where the chemical order came into effect, and the physical parameters usually exhibit transitions at the chemically stoichiometric compositions.

4. Conclusions

We comparatively investigated the thresholds in $\text{Ge}_x\text{As}_{10}\text{Se}_{90-x}$ and $\text{Ge}_x\text{Sb}_{10}\text{Se}_{90-x}$ bulk glasses. Through systematic measurements of various physical parameters like T_g , density, and refractive index, we found that, while the transition thresholds at 2.4 and 2.67 were verified in GeAsSe glasses, the replacement of As by Sb can induce the change of the transition thresholds. Further structural characterisation using Raman confirmed that, the transition threshold was correlated with the extrema of the content of the different structural units in the glasses. While the number of the structural units exhibits extrema at MCN=2.67 for GeAsSe glasses, these extrema appear in the chemically stoichiometric compositions for GeSbSe glasses.

Acknowledgements

This research is supported by the National Natural Science Foundation of China (No. 62004067), the Natural Science Foundation of Hunan Province (No. 2023JJ30438) and the Aid Program for Science and Technology Innovative Research Team in Higher Educational Institutions of Hunan Province.

References

- [1] R. P. Wang, Amorphous Chalcogenides: Advances and Applications, Pan Stanford Publisher, Singapore, 101-128 (2014); <https://doi.org/10.1201/b15599>
- [2] K. Tanaka, K. Shimakawa, Amorphous Chalcogenide Semiconductors and Related Materials, Springer International Publishing, New York, 110-121 (2011); https://doi.org/10.1007/978-1-4419-9510-0_5
- [3] L. Niu, Y. M. Chen, X. Shen, T. F. Xu, Chinese Physics B 29(8), 087803 (2020); <https://doi.org/10.1088/1674-1056/aba273>
- [4] S. W. Xu, X. N. Yang, J. H. Yang, R. X. Wang, X. Q. Su, Chalcogenide Letters 18(6), 277 (2021).
- [5] J. Kang, R. K. Kotnala, S. K. Tripathi, Chalcogenide Letters 17(12), 631 (2020); <https://doi.org/10.15251/CL.2020.1712.631>
- [6] A. P. Yang, M. Y. Sun, H. Ren, H. X. Lin, X. Feng, Z. Y. Yang, Journal of Luminescence 237, 118169 (2021); <https://doi.org/10.1016/j.jlumin.2021.118169>
- [7] P. Toronc, M. Bensoussan, A. B. Renac, Physical Review B 8(12), 5947 (1973); <https://doi.org/10.1103/PhysRevB.8.5947>
- [8] G. Lucovsky, F. L. Galeener, R. C. Keezer, R. H. Geils, H. A. Six, Physical Review B 10, 5134 (1974); <https://doi.org/10.1103/PhysRevB.10.5134>
- [9] J. C. Phillips, Journal of Non-Crystalline Solids 34(2), 153 (1979); [https://doi.org/10.1016/0022-3093\(79\)90033-4](https://doi.org/10.1016/0022-3093(79)90033-4)
- [10] J. C. Philips, Journal of Non-Crystalline Solids 43, 37(1981); [https://doi.org/10.1016/0022-3093\(81\)90172-1](https://doi.org/10.1016/0022-3093(81)90172-1)
- [11] K. Tanaka, Physical Review B 39(2), 1270 (1989); <https://doi.org/10.1103/PhysRevB.39.1270>
- [12] D. A. P. Bulla, R. P. Wang, A. Prasad, A. V. Rode, S. J. Madden, B. Luther-Davies, Applied

- Physics A 96 , 615 (2009); <https://doi.org/10.1007/s00339-009-5293-0>
- [13] X. Q. Su, R. P. Wang, B. Luther-Davies, L. Wang, Applied Physics A 113(3), 575 (2013); <https://doi.org/10.1007/s00339-013-7585-7>
- [14] R. P. Wang, A. Smith, B. Luther-Davies, H. Kokkonen, I. Jackson, Journal of Applied Physics 105, 056109 (2009); <https://doi.org/10.1063/1.3079806>
- [15] T. Wang, W. H. Wei, X. Shen, R. P. Wang, B. Luther-Davies, I. Jackson, Journal of Physics D: Applied Physics 46, 165302 (2013); <https://doi.org/10.1088/0022-3727/46/16/165302>
- [16] R. P. Wang, A. Smith, P. Amrita, D. Y. Choi, B. Luther-Davies, Journal of Applied Physics 106, 043520 (2009); <https://doi.org/10.1063/1.3204951>
- [17] W. H. Wei, R. P. Wang, X. Shen, L. Fang, B. Luther-Davies, The Journal of Physical Chemistry C 117(32), 16571 (2013); <https://doi.org/10.1021/jp404001h>
- [18] D. G. Georgoev, P. Boolchand, M. Micoulaut, Physical Review B 62, R9228 (2000); <https://doi.org/10.1103/PhysRevB.62.R9228>
- [19] G. Yang, B. Bureau, T. Rouxel, Y. Gueguen, O. Gulbiten, C. Roiland, E. Soignard, J. L. Yarger, J. Troles, J. C. Sangleboeuf, P. Lucas, Physical Review B 82(19), 195206 (2010); <https://doi.org/10.1103/PhysRevB.82.195206>
- [20] M. Reinfelde, M. Mitkova, T. Nichol, Z.G. Ivanova, J. Teteris, Chalcogenide Letters 15(1), 35 (2018).
- [21] S. W. Xu, R. P. Wang, Z. Y. Yang, L. Wang, B. Luther-Davies, Applied Physics Express 8(1), 015504 (2015); <https://doi.org/10.7567/APEX.8.015504>
- [22] S. W. Xu, L. Wang, X. Shen, Acta Physica Sinica 64(22), 223302 (2015); <https://doi.org/10.7498/aps.64.223302>
- [23] G. Saffarini, Solid State Communications 91, 577 (1994); [https://doi.org/10.1016/0038-1098\(94\)90378-6](https://doi.org/10.1016/0038-1098(94)90378-6)
- [24] A. Giridhar, P. S. L. Narasimhan, S. Mahadevan, Journal of Non-Crystalline Solids 43, 29 (1981); [https://doi.org/10.1016/0022-3093\(81\)90171-X](https://doi.org/10.1016/0022-3093(81)90171-X)
- [25] G. Opletal, D. W. Drumm, T. C. Petersen, R. P. Wang, S. P. Russo, The Journal of Physical Chemistry A 119(24), 6421 (2015); <https://doi.org/10.1021/acs.jpca.5b00039>